Modelling flow in the porous bottom of the Barents Sea shelf

doi:10.5697/oc.55-1.129
OCEANOLOGIA, 55 (1), 2013.
pp. 129–146.

KEYWORDS
Porous media
Surface waves
Tides
Ekman layer

Stanisław R. Massel

Institute of Oceanology,
Polish Academy of Sciences,
Powstańców Warszawy 55, Sopot 81–712, Poland;

e-mail: smas@iopan.gda.pl

Received 18 October 2012, revised 21 November 2012, accepted 26 November 2012.

Abstract

In their recent paper, Węsławski et al. (2012) showed that the Svalbardbanken area of the Barents Sea is characterized by a high organic carbon settlement to the permeable sea bed, which consists of gravel and shell fragments of glacial origin. In the present paper, which can be considered as a supplement to the Węsławski et al. paper, two potential hydrodynamic mechanisms of downward pore water transport into porous media are discussed in detail. In particular, estimated statistical characteristics of the pore water flow, induced by storm surface waves, indicate that the discharge of water flow can be substantial, even at large water depths. During stormy weather (wind velocity $V = 15$ m s^{-1} and wind fetch $X = 200$ km) as much as 117.2 and 26.1 m^3 hour^{-1} of water filter through the upper 5 m of the shell pit at water depths of 30 and 50 m respectively. For a porous layer of greater thickness, the mean flow discharge is even bigger.

The second possible mechanism of flow penetration in the porous layer is based on the concept of geostrophic flow and spiral formation within the Ekman layer. Assuming that the current velocity in the near-bottom water layer is $\overline{u} = 1$ m, the resulting mean discharge through this layer becomes as large as 0.99 and 0.09 m^3 s^{-1} for downstream and transverse flows respectively.

1. Introduction

In a recently published interesting paper, Węsławski et al. (2012) suggested that the Spitsbergenbanken may be acting as a huge sink for organic carbon owing to the substantial permeability of the sediments. This area is a large converter, capable of processing a significant part of the primary production below the seabed surface and enriching the surrounding waters with regenerated nutrients. The sea bed in this area is covered with loose carbonate material: barnacles, molluscs, and a mix of very coarse sand and gravel. The resulting permeability of the sediments (av $= 4.28 \times 10^{-10}$ m^2) is well above the permeability of comparable sands of the order of 10^{-12} m^2 for an average sand grain diameter of 250 μm.

Węsławski et al. (2012) mentioned some modelling results in their paper, but without making reference to the assumptions and methods applied. It is clear that modelling results are very sensitive to the values of the critical parameters used in calculations. The interpretation of the results of calculations should therefore be considered from this perspective. In the present paper, two potential hydrodynamic mechanisms, which may be responsible for the penetration of flow into highly porous media, are presented in detail. Firstly, the flow in porous media due to high ocean surface waves is discussed and the discharge of the flow penetrating into the porous layer is estimated. Secondly, the structure of the frictional layer of the geostrophic flow appearing in a porous bottom due to the Earth's rotation is described. The flow structure, similar to the Ekman spiral, induces a discharge of pore water with attenuating velocity. The theoretical results are illustrated by examples of calculations of some velocity profiles and flow discharges for selected porous layer characteristics, and wave and current parameters.

2. Material and methods

2.1. Porous media characteristics

The porous layer in the Spitsbergenbanken area is made up largely of loose carbonate material. Samples of sediment and benthos collected with a van Veen grab and dredge showed that the mean sediment grain diameter was $D = 0.02$ m, and that the porosity of the mixture of shells, stones and gravel $n = 0.39$. The intrinsic permeability K, determined by Klute & Dirksen (1986), ranges from 3.5 to 5.4×10^{-10} m^2 with a mean value of 4.28×10^{-10} m^2. This permeability is well above the permeabilities of comparable Baltic sands, which are of the order of 10^{-12}–10^{-11} m^2.

In practice, the relationship between the permeability K and the grain diameter D is often used, namely $K = C \times D^2$. Harleman et al. (1963)

suggested that $C = 6.54 \times 10^{-4}$ (D is expressed in [cm] and K in [cm^2]). Therefore, for $D = 2.0$ cm, we obtain $K = 2.62 \times 10^{-3}$ cm^2 $= 2.62 \times 10^{-7}$ m^2. This value is very different from the Klute & Dirksen (1986) estimate.

In the following calculations, the hydraulic conductivity K_f rather than the intrinsic permeability K is used. These two quantities are related by the following formula

$$K_f = \frac{g}{\nu} K, \tag{1}$$

where $\nu = 1.06 \times 10^{-6}$ m^2 s^{-1}.

Substituting the permeability value given by Harleman et al. (1963) into eq. (1) we obtain $K_f = 2.47$ m s^{-1}.

Bear (1972) in his Table 5.5.1 gives a summary of the hydraulic conductivity and permeability of various bottom materials: the value for clean gravel is $10^{-2} < K_f < 10^{0}$ m s^{-1}, and that for clean sand or sand and gravel is $10^{-5} < K_f < 10^{-2}$ m s^{-1}. For a given sediment diameter Bear suggested the following experimental relationship between the hydraulic conductivity and the sediment diameter D:

$$K_f = 6500\, D^2, \tag{2}$$

where D is expressed in [m] and K_f is in [m s^{-1}]. After substituting the mean sediment diameter $D = 0.02$ m, we obtain $K_f \approx 2.6$ m s^{-1}. This value appears to be very close to the estimate of Harleman et al. (1963). Therefore, a hydraulic conductivity of $K_f \approx 2.5$ m s^{-1} will be used in the following calculations. Similar values of the hydraulic conductivity of gravel were obtained in the outflow experiment reported by Sanford et al. (1995).

2.2. Pore water circulation due to wind-induced surface waves

The meteorological conditions in the Barents Sea are dominated by cyclones that form in the North Atlantic and move into the Barents Sea from the south-west, which is the sector with the longest wave-generating fetches. There is little variation in the mean significant wave height in the western Barents Sea, but the wave height decreases eastwards. The highest significant wave height recorded at the AMI location was 12.7 m on 31 October 1997 during south-westerly winds caused by a rapidly developing area of low pressure moving from Jan Mayen into the Barents Sea. At the Nordkapbanken, the highest significant wave height of 13.6 m was recorded during a severe storm on 3 January 1993.

To estimate the local velocity of water flow in the porous layer of Svalbardbanken, let us apply the general model for multiphase flow in porous media (Massel et al. 2004, 2005). However, for conditions in the region between Bjornoya and Hopen in the Barents Sea, this general model

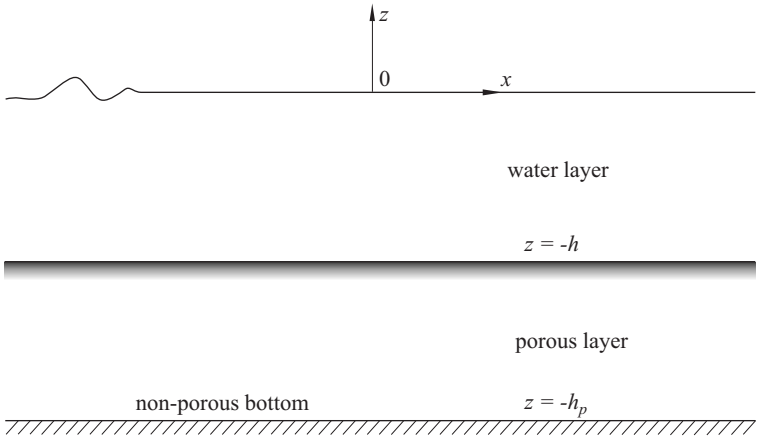

Figure 1. Reference scheme

can be much simplified by assuming that the porous layer is fully saturated by water. Let the water depth be constant ($= h$) and the thickness of the porous layer be $(h_p - h)$, where h_p is the depth of the non-porous bottom (see Figure 1). We assume additionally that surface waves are characterized by the JONSWAP spectrum (Massel 1999).

$$S(\omega) = \alpha g^2 \omega^{-5} \exp\left[-\frac{5}{4}\left(\frac{\omega}{\omega_p}\right)^{-4}\right] \gamma^{\delta}, \tag{3}$$

where

$$\alpha = 0.076\left(\frac{gX}{V^2}\right)^{-0.22}, \tag{4}$$

$$\omega_p = 7\pi \left(\frac{g}{V}\right)\left(\frac{gX}{V^2}\right)^{-0.33}, \tag{5}$$

$$\delta = \exp\left[-\frac{(\omega - \omega_p)^2}{2\sigma_0^2 \omega_p^2}\right], \tag{6}$$

in which V is the wind velocity, X is the wind fetch, ω_p is the spectrum peak frequency, the peakedness parameter $\gamma = 3.3$ and parameter $\sigma_0 = 0.07$ for $\omega < \omega_p$, and $\sigma_0 = 0.09$ for $\omega > \omega_p$.

The directional characteristics of the surface waves in this area are not known. For simplicity, therefore, we assume that the waves are propagating in one direction, along the x axis with very narrow directional spreading.

The surface waves induce pore water flow in the porous layer. For a layer completely saturated by water, this flow is controlled by the Laplace equation in the vertical plane (x, z). Thus we have

$$\frac{\partial^2 p}{\partial x^2} + \frac{\partial^2 p}{\partial z^2} = 0. \tag{7}$$

The solution to the above equation with proper boundary conditions becomes (Massel et al. 2005)

$$p(x,z,t) = \Re\left\{\rho_w g \int_0^\infty \frac{\cosh[k(z+h_p)]}{\cosh(kh)\cosh[k(h_p-h)]}\,\exp[i(kx-\omega t)]\,dA(\omega)\right\}, \tag{8}$$

where ρ_w is the water density, and the increments of the random amplitudes $dA(\omega)$ are related to the sea surface spectrum $S(\omega)$ as follows:

$$\overline{dA(\omega)dA\,(\omega_1)} = S(\omega)\,\delta(\omega-\omega_1)\,d\omega\,d\omega_1, \tag{9}$$

where $\delta(x)$ is the Dirac delta.

For the conditions at the Svalbardbanken we can assume, moreover, that the horizontal and vertical velocities of the pore water satisfy Darcy's law, i.e.

$$\left.\begin{aligned} u(x,z,t) &= -\frac{K_f}{\rho_w g}\,\frac{\partial p}{\partial x} \\ w(x,z,t) &= -\frac{K_f}{\rho_w g}\,\frac{\partial p}{\partial z} \end{aligned}\right\}, \tag{10}$$

Therefore we have

$$u(x,z,t) = \\ = -\Re\left\{iK_f \int_0^\infty \frac{k\cosh[k(z+h_p)]}{\cosh(kh)\cosh[k(h_p-h)]}\exp[i(kx-\omega t)]dA(\omega)\right\}, \tag{11}$$

and

$$w(x,z,t) = \\ = -\Re\left\{K_f \int_0^\infty \frac{k\sinh[k(z+h_p)]}{\cosh(kh)\cosh[k(h_p-h)]}\,\exp[i(kx-\omega t)]dA(\omega)\right\}, \tag{12}$$

From the above equations it follows that the standard deviations of the velocities u and w in the porous media are (for simplicity, it was assumed that $x = 0$)

$$\sigma_u(z) = K_f\left\{\int_0^\infty \left[\frac{k\cosh[k(z+h_p)]}{\cosh(kh)\cosh[k(h_p-h)]}\right]^2 S(\omega)\,d\omega\right\}^{1/2} \tag{13}$$

and

$$\sigma_w(z) = K_f \left\{ \int_0^\infty \left[\frac{k \sinh[k(z+h_p)]}{\cosh(kh)\cosh[k(h_p-h)]} \right]^2 S(\omega)\, d\omega \right\}^{1/2}. \tag{14}$$

Using standard deviations we can calculate some statistical characteristics of the pore water velocities, which are in fact random quantities. The initial point for the statistical analysis is the assumption that the probability density function for the sea surface displacements $\zeta(t)$ is a Gaussian one, i.e.

$$f(\zeta) = \frac{1}{\sqrt{2\pi}\,\sigma_\zeta} \exp\left[-\frac{(\zeta - \overline{\zeta})^2}{2\sigma_\zeta^2} \right], \tag{15}$$

where $\overline{\zeta}$ is the mean value and σ_ζ is the standard deviation.

We assume that the Gaussian distribution is also valid for the wave-induced pore water velocities. Thus, for the horizontal $u(t)$ and vertical $w(t)$ components of the flow in porous media we have

$$f(u(z)) = \frac{1}{\sqrt{2\pi}\,\sigma_u(z)} \exp\left(-\frac{(u-\overline{u})^2(z)}{2\sigma_u^2(z)} \right) \tag{16}$$

and

$$f(w(z)) = \frac{1}{\sqrt{2\pi}\,\sigma_w(z)} \exp\left(-\frac{(w-\overline{w})^2(z)}{2\sigma_w^2(z)} \right). \tag{17}$$

It is clear that the mean values of both velocities are zero, i.e.

$$\overline{u}(z) = \int_{-\infty}^{\infty} \frac{u}{\sqrt{2\pi}\sigma_u(z)} \exp\left[-\frac{u^2}{2\sigma_u^2(z)} \right] du = 0 \tag{18}$$

and

$$\overline{w}(z) = \int_{-\infty}^{\infty} \frac{w^2}{\sqrt{2\pi}\sigma_w(z)} \exp\left[-\frac{w^2}{2\sigma_w^2(z)} \right] dw = 0. \tag{19}$$

For making a practical estimate of the flow discharge within the porous layer, the module of the velocity $U(z,t)$ becomes an important quantity. Thus we have

$$U(z,t) = \sqrt{u^2(z,t) + w^2(z,t)}. \tag{20}$$

It should be noted that the direction of the instantaneous velocity $U(z,t)$ makes an oblique angle $\theta(z,t)$ with the vertical axis given by

$$\theta(z,t) = \arctan\left(\frac{\sigma_u(z)}{\sigma_w(z)} \right). \tag{21}$$

The velocity $U(z,t)$ is a random quantity with the following probability density function (Papoulis 1965):

$$f(U(z)) = \frac{U(z)}{\sigma_u(z)\sigma_w(z)} I_0(m_1 U^2) \exp(-m_2 U^2), \tag{22}$$

where I_0 is a Bessel function of the second kind and zero order. The functions $m_1(z)$ and $m_2(z)$ are given by the following relationships (Papoulis 1965):

$$m_1(z) = \frac{\sigma_u^2(z) - \sigma_w^2(z)}{4\sigma_u^2(z)\sigma_w^2(z)}, \tag{23}$$

$$m_2(z) = \frac{\sigma_u^2(z) + \sigma_w^2(z)}{4\sigma_u^2(z)\sigma_w^2(z)}. \tag{24}$$

Therefore, the mean value of the velocity module for a particular water depth z becomes

$$\overline{U}(z) = \frac{1}{\sigma_u(z)\sigma_w(z)} \int_0^\infty U^2 I_0(m_1 U^2) \exp(-m_2 U^2) dU. \tag{25}$$

Finally, let us define the total mean velocity $\hat{U}$ and the mean discharge M of flow through a porous layer of thickness $(h_p - h)$ by integrating the mean module velocity $\overline{U}(z)$ over z. Thus we have

$$\hat{U} = \frac{1}{h_n - h} \int_{-h_n}^{-h} \overline{U}(z) dz. \tag{26}$$

Hence, the mean discharge of flow through the surface of one square metre in one hour is

$$\hat{M} = \hat{U} \times 1\,\mathrm{m}^2 \times 3600 \quad \text{in} \quad [\mathrm{m}^3\,\mathrm{hour}^{-1}]. \tag{27}$$

2.3. Pore water circulation due to tidal currents

The second mechanism that may be responsible for pore water circulation in the porous layer in the Svalbardbanken area is due to tidal currents and bottom Ekman layer formation. The tides in the Barents Sea are particularly interesting since the major tidal constituents have amphidromic structures within the area. For example, the main amphidromic point of constituent M_2 is located south-east of Bear Island. This leads to somewhat larger M_2 amplitudes observed over Svalbardbanken (Gjevik et al. 1994, Kowalik & Proshutinsky 1995). Kowalik & Proshutinsky, in particular, using a high-resolution grid, showed a well-developed trapped motion with a distinctive tidal oscillatory character in the Bear Island-Spitsbergenbanken

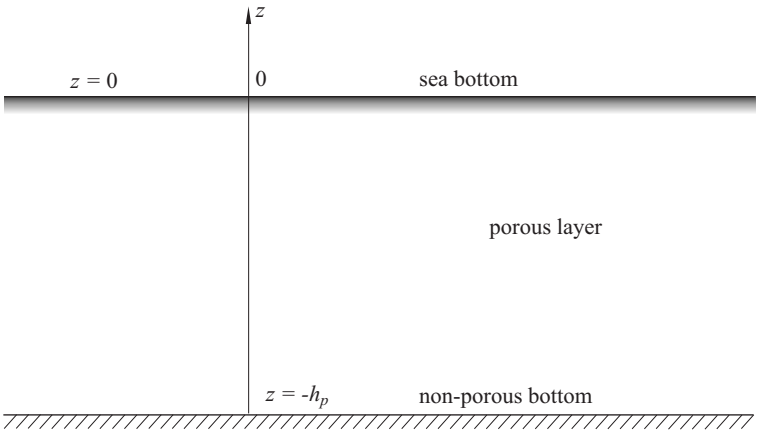

Figure 2. Coordinate system for a porous layer

domain. Calculations with a resolution of 4.63 km confirm the existence of mixed tidal currents due to eight tidal constituents with an amplitude of up to $0.8 - 1.0$ m s^{-1}.

Let us consider for a moment the motion of the particular tidal constituent as the motion of a very long wave. For example, the most important M_2 constituent has a period of $T = 12.42$ hours. This means that the corresponding wave number k is $\approx 6.3 \times 10^{-6}$ m^{-1} for a water depth $h = 50$ m. If we neglect the Earth's rotation, the horizontal and vertical velocities due to tidal waves become (Massel et al. 2005)

$$u(x,z,t) \approx K_f \frac{k\cosh[k(z+h_p)]}{\cosh[k(h_p-h)]} \approx 10^{-5} \quad [\mathrm{m\,s^{-1}}], \tag{28}$$

$$w(x,z,t) \approx K_f \frac{k\sinh[k(z+h_p)]}{\cosh[k(h_p-h)]} \approx 10^{-5} \quad [\mathrm{m\,s^{-1}}]. \tag{29}$$

Both velocities are negligibly small and can be ignored, except perhaps in the boundary layer close to the sea bottom at $z = -h$, as in the close proximity of the porous bed, a viscous boundary layer of thickness δ of the order $\mathcal{O}(\sqrt{\nu/\omega})$ forms in which the flow can be considered as essentially horizontal. In our case, for long waves of the period $T = 12.42$ hours, $\delta =$ ca 0.08 m.

In general, circulation in the porous layer in the Svalbardbanken area can be induced by the tidal current, when the Earth's rotation is taken into account, and the Ekman bottom layer is formed. Let us therefore consider a uniform, geostrophic flow in a homogeneous fluid over a flat porous bottom with velocity $\overline{u}$, corresponding to the semidiurnal tidal current, which dominates the diurnal current (Figure 2). Following Danielson & Kowalik

(2005) it is assumed that the velocity is a combination of the zero-order geostrophic solution (u_0, v_0) and the first-order solution (u_0, v_0) representing changes due to friction. For the zero-order solution we have the following set of equations:

$$\left.\begin{aligned} \frac{\partial u_0}{\partial t} - fv_0 &= -g\frac{\partial \zeta}{\partial x} \\ \frac{\partial v_0}{\partial t} + fu_0 &= -g\frac{\partial \zeta}{\partial y} \end{aligned}\right\}, \tag{30}$$

while for the first-order solution these equations are

$$\left.\begin{aligned} \frac{\partial u_1}{\partial t} - fv_1 &= A_z\frac{\partial^2 u_1}{\partial z^2} \\ \frac{\partial v_1}{\partial t} + fu_1 &= A_z\frac{\partial^2 v_1}{\partial z^2} \end{aligned}\right\}, \tag{31}$$

where ζ is the surface elevation, f is the Coriolis parameter $f = 2\Omega \sin\phi$, where the Earth's rotational frequency $\Omega = 7.25 \times 10^{-5}$ rad s^{-1}, ϕ is the latitude of a given location and A_z is the eddy viscosity coefficient.

As we are interested only in a rough estimate of the pore water circulation, we shall make some simplifications to the above equations. First of all we assume that for a short period of time, the time gradients can be neglected and that the motion can be treated as stationary. Also, in the close vicinity of the point of observation, the spatial surface gradients are negligibly small: thus $u_0 = v_0 = 0$. Furthermore, we assume that the direction of flow near the bottom coincides with the x axis.

Owing to the high permeability of porous material, the flow penetrates into the porous layer and becomes influenced by the Coriolis force. Taking into account the above simplifications, the governing equations of motion in the porous layer take the form (Pedlosky 1987, Cushman-Rosin 1994, Danielsen & Kowalik 2005)

$$\left.\begin{aligned} -fv &= A_z\,\frac{d^2u}{dz_1^2} \\ f(u-\bar{u}) &= A_z\,\frac{d^2v}{dz_1^2} \end{aligned}\right\}, \tag{32}$$

where u and v are the horizontal components of the final flow velocity.

The general solution of the system of eqs. (32) takes the form

$$\frac{u-\overline{u}}{\overline{u}} \;=\; C_1 \exp\left[(1+i)\frac{z_1}{\delta_p}\right] + C_2 \exp\left[(1-i)\frac{z_1}{\delta_p}\right] +$$

$$+ \quad C_3 \exp\left[-(1+i)\frac{z_1}{\delta_p}\right] + C_4 \exp\left[-(1-i)\frac{z_1}{\delta_p}\right] \tag{33}$$

and

$$\begin{aligned} \frac{iv}{\overline{u}} &= C_1 \exp\left[(1+i)\frac{z_1}{\delta_p}\right] - C_2 \exp\left[(1-i)\frac{z_1}{\delta_p}\right] + \\ &+ C_3 \exp\left[-(1+i)\frac{z_1}{\delta_p}\right] - C_4 \exp\left[-(1-i)\frac{z_1}{\delta_p}\right], \end{aligned} \tag{34}$$

where the so-called Ekman layer thickness for stationary motion becomes

$$\delta_p = \sqrt{\frac{2A_z}{f}}. \tag{35}$$

The unknown complex coefficients C_1, C_2, C_3 and C_4 should be determined from the boundary conditions at $z_1 = 0$ and $z_1 = h_p$. In particular, for $z_1 = 0\,(z = -h_p)$ velocities u and v should both be equal to 0, and at the porous sea bottom $z_1 = h_p, (z = 0)$, velocities u and v must be equal to $u = \overline{u}$ and $v = 0$ respectively. Therefore, after substitution of eqs. (33) and (34) into these boundary conditions we obtain

$$C_1 = \frac{\exp\left[-2(1+i)\dfrac{h_p}{\delta_p}\right]}{2\left(1 - \exp\left[-2(1+i)\dfrac{h_p}{\delta_p}\right]\right)}, \tag{36}$$

$$C_2 = \frac{\exp\left[-2(1-i)\dfrac{h_p}{\delta_p}\right]}{2\left(1 - \exp\left[-2(1-i)\dfrac{h_p}{\delta_p}\right]\right)}, \tag{37}$$

$$C_3 = \frac{-1}{2\left(1 - \exp\left[-2(1+i)\dfrac{h_p}{\delta_p}\right]\right)}, \tag{38}$$

$$C_4 = \frac{-1}{2\left(1 - \exp\left[-2(1-i)\dfrac{h_p}{\delta_p}\right]\right)}. \tag{39}$$

It should be noted that for a porous layer of infinite thickness ($h_p = \infty$), the solution to the problem is much simplified. Hence for coefficients C we obtain $C_1 = C_2 = 0$ and $C_3 = C_4 = -1/2$, and the velocities now become

$$\left.\begin{aligned} u(z) &= \overline{u}\left[1 - \exp\left(-\frac{z_1}{\delta_p}\right)\cos\left(\frac{z_1}{\delta_p}\right)\right] \\ v(z) &= \overline{u}\exp\left(-\frac{z_1}{\delta_p}\right)\sin\left(\frac{z_1}{\delta_p}\right) \end{aligned}\right\}. \tag{40}$$

The above solution is in agreement with the ones obtained by Pedlosky (1987) and Cushman-Rosin (1994). In this case, very close to the non-porous bottom ($z_1 \to 0$), the transverse flow v is equal to the downstream velocity ($v \sim u \sim \frac{\bar{u}z_1}{\delta_p}$). Therefore the resulting flow vector is directed at 45 from the interior flow.

When we integrate both velocity components over the z axis we obtain the mean discharge of flow through the porous layer per unit width for a given tidal current as follows:

– downstream flow

$$M_u = \frac{1}{h_p}\int_0^{h_p} u(z_1)dz_1, \tag{41}$$

– transverse flow

$$M_v = \frac{1}{h_p}\int_0^{h_p} v(z_1)dz_1. \tag{42}$$

3. Results and discussion

To obtain some insight into predicted flow velocity and discharge over the Barents Sea shelf, some simulations were done using the theoretical formulae developed in the previous Sections. In particular, the four specific cases mentioned by Węsławski et al. (2012) were considered. However,

Table 1. Wind parameters and flow discharge due to surface waves

Case	h [m]	h_p [m]	$(h_p - h)$ [m]	V [m s^{-1}]	X [km]	$\hat{M}$ [m^3 hour^{-1}]
1	30	35	5	15	200	117.2
2	30	50	20	15	200	99.0
3	50	55	5	15	200	26.1
4	50	70	20	15	200	21.0

only one sediment diameter $D = 0.02$ m was used in the calculations. The characteristic depths h and h_p, as well as the wind parameters are given in Table 1. A hydraulic conductivity of $K_f = 2.5$ m s^{-1} was assumed in all the calculations.

Figures 3–6 show the vertical profiles of the standard deviations of both horizontal components u and v as well as the module of velocity vector $\overline{U}$.

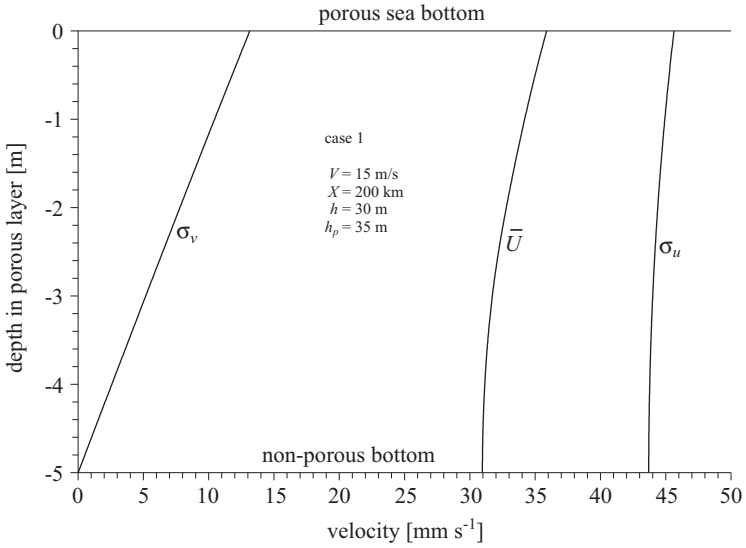

Figure 3. Standard deviations and mean velocity profiles for Case 1

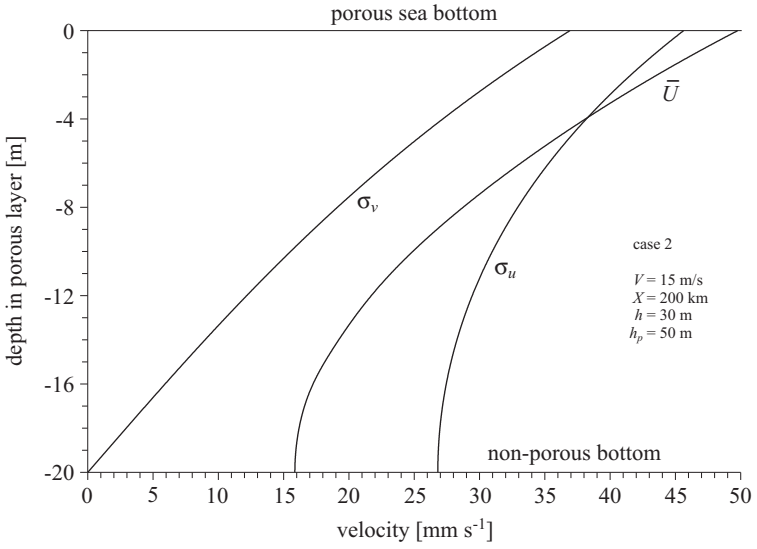

Figure 4. Standard deviations and mean velocity profiles for Case 2

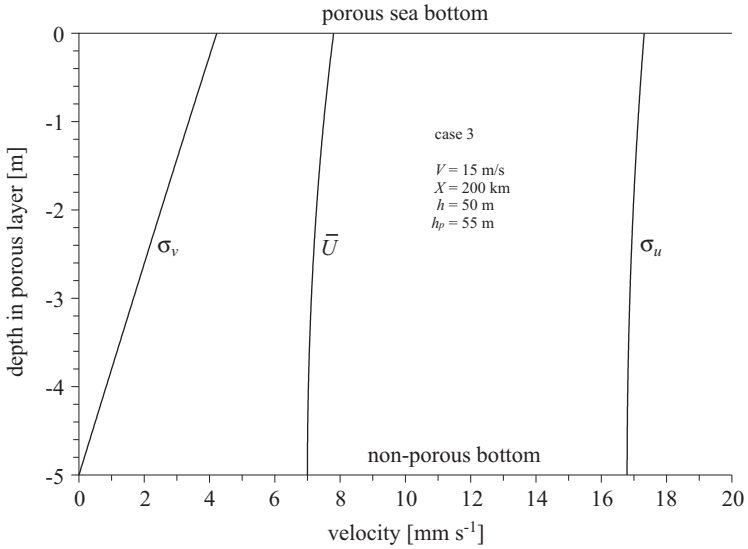

Figure 5. Standard deviations and mean velocity profiles for Case 3

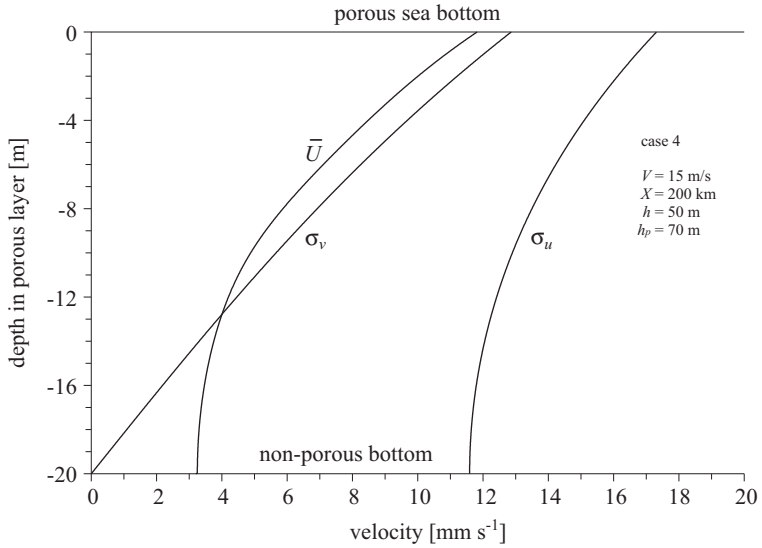

Figure 6. Standard deviations and mean velocity profiles for Case 4

When the thickness of the porous layer is small (Case 1 (see Figure 3) and Case 3 (see Figure 5)), the flow velocities are very uniform. The standard deviation σ_u changes a little in the vertical direction while σ_v attenuates linearly in the porous layer.

The mean module of the velocity vector $\overline{U}(z)$ (see eq. (25)) is also given

in Figures 3–6. Again, for a small porous layer thickness this does not change substantially with depth. For a porous layer thickness of 20 m, velocity $\overline{U}(z)$ attenuates with depth and its value at the non-porous depth depends on the water layer thickness. However, even for a water depth $h = 50$ m, $\overline{U}(z)$ is still > 3 mm s^{-1}.

The mean flow discharge $\hat{M}$, based on the mean module velocity $\overline{U}$, is summarized for all cases in Table 1 in m^3 hour^{-1}. For Case 1 (shallow water depth, small porous layer thickness) $\hat{M} = 117.2$ m^3 hour^{-1}, while for the same porous layer thickness but for deeper water (Case 3), the mean flow discharge is only 26.1 m^3 hour^{-1}.

When the porous layer is thicker (Case 2 and 4), the standard deviations σ_u and σ_v, as well as the mean total velocity $\bar{U}$ change distinctly with depth (see Figures 4 and 6). As in the case of a thin porous layer, the mean flow discharge depends on the water depth and for Cases 2 and 4, it is equal to 99.0 and 21.0 m^3 hour^{-1} respectively. The relationships of the flow discharges for thicker or thinner porous layers reflect the fact that velocity attenuation is more intensive in the upper part of the porous layer.

In Section 2.3, it was shown that the geostrophic flow in the water layer penetrates into porous media and forms an Ekman-type spiral. Each layer of pore water is retarded by friction with the layer beneath it and the stresses within the pore water layer are communicated from one lamina to another. The resulting pore water velocity vector gradually turns as the non-porous bottom is approached. The thickness of the Ekman layer δ_p depends strongly on the eddy viscosity coefficient A_z (see eq. (33)). This coefficient A_z for flow in a porous media is not known. However, it is quite reasonable to consider the eddy viscosity coefficient A_z as a function of the Reynolds number, $\mathrm{Re} \approx \frac{U \times D}{\nu}$, where U is the characteristic velocity, D is the sediment grain diameter and $\nu = 1.0 \times 10^{-6}$ m^2 s^{-1} is the coefficient of molecular viscosity. In oceanic water columns coefficient A_z is much larger than the molecular viscosity. Values of $A_z \approx 10^{-3} - 10^{-2}$ m^2 s^{-1} are usually used in the hydrodynamic models. Water flow in the porous layer is less turbulent than in the water layer. On the other hand, owing to the considerable permeability of the porous material, the flow in the porous layer cannot be considered laminar. As the relationship between coefficient A_z and the Reynolds number for flow in the porous layer is still unknown, the values of $A_z = 10^{-5} - 10^{-2}$ m^2 s^{-1}, used in the calculations, seem to be a reasonable compromise.

Let us therefore assume that the latitude of the point under consideration in the Barents Sea is $\phi = 75°$. The porous layer thicknesses h_p are listed in Table 2. The current velocity at the sea bottom induced by tides is assumed to be equal to $\overline{u} = 1$ m s^{-1} and directed along the x axis. The

Table 2. Mean discharges in the porous layer in the Ekman spiral

Case	A_z [m^2 s^{-1}]	Mean discharge [m^3 s^{-1}]	
		downstream flow	transverse flow
1	10^{-3}	0.55	0.65
thickness:	10^{-4}	0.88	0.62
$h_p = 5$ m	10^{-5}	0.96	0.18
2	10^{-3}	0.91	0.09
thickness:	10^{-4}	0.97	0.03
$h_p = 20$ m	10^{-5}	0.99	0.009

pattern of the vertical profiles depends strongly on the value of A_z and in consequence on the Ekman layer thickness δ_p. The thickness δ_p changes from $\delta_p = 3.78$ m for $A_z = 10^{-3}$ m^2 s^{-1}, to $\delta_p = 1.19$ m for $A_z = 10^{-4}$ m^2 s^{-1} and $\delta_p = 0.38$ m for $A_z = 10^{-5}$ m^2 s^{-1}.

In Figure 7, the vertical profiles of both horizontal components of the Ekman spiral, i.e. u and v are shown for a thin porous layer (Cases 1 and 3). In the figure the symbol n denotes the power in the expression for the eddy viscosity coefficients, i.e. $A_z = 10^{-n}$ m^2 s^{-1}, where $n = 3, 4, 5$.

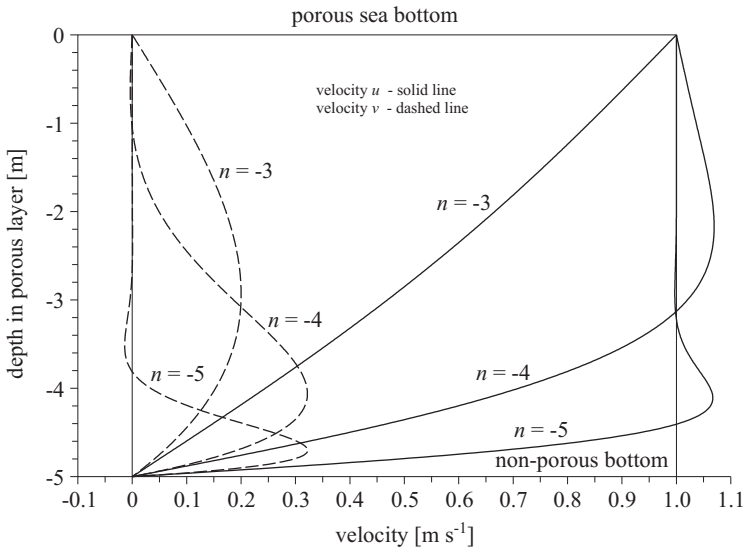

Figure 7. Vertical profiles of velocities u and v for a shallow porous layer ($h_p = 5$ m)

Figure 8 ilustrates the vertical profiles of a porous layer of greater thickness (Cases 2 and 4). The same three values of the eddy viscosity

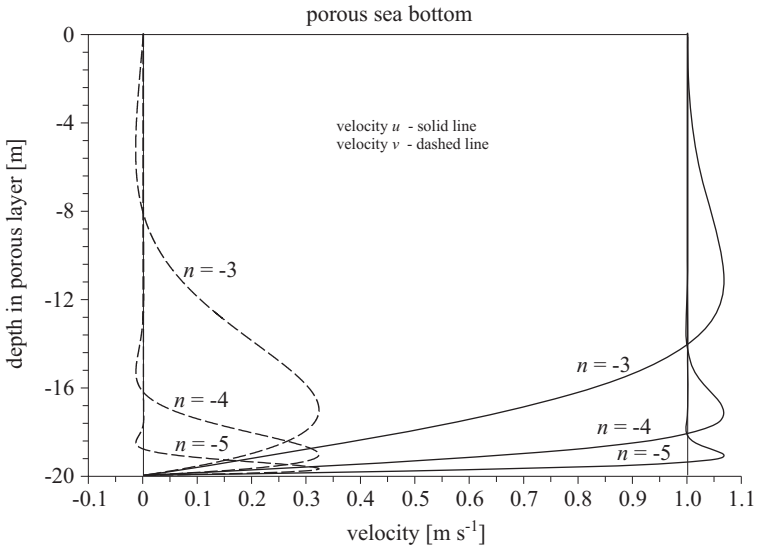

Figure 8. Vertical profiles of velocities u and v for a deeper porous layer (h_p = 20 m)

coefficients A_z have been used. As in the previous case, the thickness of the Ekman spiral decreases with decreasing coefficient A_z.

Additionally, in Figure 9, the velocity vector as a function of coordinate z is given for the greater thickness. The tip of the velocity vector traces a spiral as z decreases to $z = -h_p$ value.

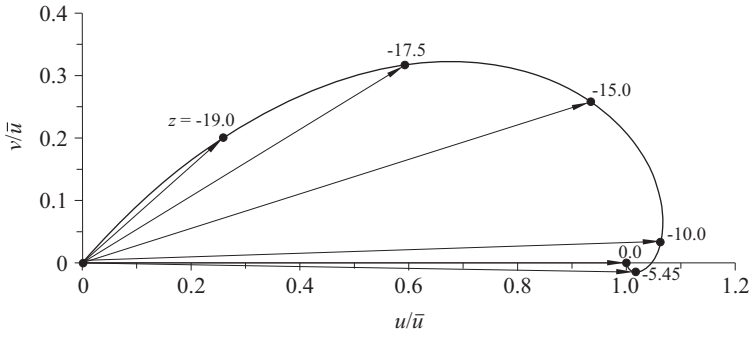

Figure 9. The velocity vector within the Ekman layer. The locus of the tip of the velocity vector traces the Ekman spiral. The value of depth z corresponding to each vector is indicated on the spiral curve

When we integrate the vertical velocity profiles we obtain the discharges through the entire porous layer per unit width. Mean discharges M_u

(downstream flow) and M_v (transverse flow) calculated by eqs. (41) and (42), are summarized in Table 2.

The results obtained in this paper appear to be different from those given by Węsławski et al. (2012). First of all, the present results are related to the mean values of the flow velocities and discharges in contrast to the root-mean-square values used in the former paper. Additionally, the mean sediment diameter D was fixed and equal to 0.02 m. As a consequence, the hydraulic conductivity K_f, estimated by a Bear-type relationship, is equal to 2.5 m s^{-1}. Assuming the JONSWAP spectra and the validity of Darcy's law, the calculated mean values of the mean module velocity and mean flow discharge show that the pore water flow due to high permeability can penetrate very deep into porous media.

The second possible flow mechanism in the form of a bottom Ekman layer appears to be very successful in transporting pore water into the porous layer. The flow discharges are higher than for the case of surface-wave induced flow. Substantial attenuation of both velocity components is observed only within the Ekman layer. Above this layer, the downstream velocity in particular remains rather high, while the transverse velocity approaches zero close to the sea bottom.

Summarizing the above discussion we may suggest that both presented flow mechanisms in the highly porous bottom of the Svalbardbanken area in the Barents Sea are capable of transporting a substantial amount of water into the porous layer. The first suggested mechanism is related to stormy surface waves, while the second one depends on the geostrophic flow and Ekman bottom layer formation. The results are purely theoretical, so direct measurements in the sediment layer are of vital importance for the proper description of the pore water flow in the sediments in the Svalbardbanken region.

References

Bear J., 1972, *Dynamics of fluids in porous media*, Elsevier, Dover, New York, 764 pp.

Cushman-Roisin B., 1994, *Introduction to geophysical fluid dynamics*, Prentice Hall, Englewood Cliffs, 320 pp.

Danielson S., Kowalik Z., 2005, *Tidal currents in the St. Lawrence Island region*, J. Geophys. Res., 110, C10004, http://dx.doi.org/10.1029/2004JC002463.

Gjevik B., Nost E., Straume T., 1994, *Model simulations of the tides in the Barents Sea*, J. Geophys. Res., 99 (C2), 3337–3350, http://dx.doi.org/10.1029/93JC02743.

Klute A., Dirksen C., 1986, *Hydraulic conductivity and diffusivity: laboratory methods*, [in:] *Methods of soil analysis. Part 1. Physical and mineralogical*

methods, Agronomy Monograph No. 9, 2nd edn., Am. Soc. Agronom., Madison, WI, 687–734.

Kowalik Z., Proshutinsky A. Yu., 1995, *Topographic enhancement of tidal motion in the western Barents Sea*, J. Geophys. Res., 100 (C2), 2613–2637, http://dx.doi.org/10.1029/94JC02838.

Massel S. R., 1999, *Fluid mechanics for marine ecologists*, Springer, Heidelberg, 566 pp., http://dx.doi.org/10.1007/978-3-642-60209-2.

Massel S. R., Przyborska A., Przyborski M., 2004, *Attenuation of wave-induced groundwater pressure in shallow water. Part 1*, Oceanologia, 46 (3), 383–404.

Massel S. R., Przyborska A., Przyborski M., 2005, *Attenuation of wave-induced groundwater pressure in shallow water. 2. Theory*, Oceanologia, 47 (3), 281–323.

Papoulis A., 1965, *Probability, random variables and stochastic processes*, McGraw-Hill Book Co., New York, 583 pp.

Sanford W. E., Steenhuis T. S., Parlange J.-Y., Surface J. M., Peverly J. H, 1995, *Hydraulic conductivity of gravel and sand as substrates in rock-reed filters*, Ecol. Eng., 4 (4), 321–336, http://dx.doi.org/10.1016/0925-8574(95)00004-3.

Węsławski J. M., Kędra M., Przytarski J., Kotwicki L., Ellingsen I., Skardhamar J., Renaud P., Goszczko I., 2012, *A huge biocatalytic filter in the centre of Barents Sea shelf?*, Oceanologia, 54 (2), 325–335, http://dx.doi.org/10.5697/oc.54-2.325.